Synthesis and Characterization of quasi-two-dimensional nano-flakes of the Kitaev Magnets α-$RuCl_3$ and Na_2IrO_3.

Pardeep Kumar

A dissertation submitted for the partial fulfilment
of BS-MS dual degree in Science

Indian Institute of Science Education and Research Mohali
April 2019

Certificate of Examination

This is to certify that the dissertation titled **Synthesis and Characterization of quasi-two-dimensional nano-flakes of the Kitaev Magnets α-$RuCl_3$ and** Na_2IrO_3 submitted by **Pardeep Kumar** (Reg. No. MS14076) for the partial fulfillment of BS-MS dual degree programme of the Institute, has been examined by the thesis committee duly appointed by the Institute. The committee finds the work done by the candidate satisfactory and recommends that the report be accepted.

Dr. G. Sheet | Dr. Sanjeev Kumar | Dr. Yogesh Singh (Supervisor)

Dated: April 26, 2019

Declaration

The work presented in this dissertation has been carried out by me under the guidance of Dr. Yogesh Singh at the Indian Institute of Science Education and Research Mohali.

This work has not been submitted in part or in full for a degree, a diploma, or a fellowship to any other university or institute. Whenever contributions of others are involved, every effort is made to indicate this clearly, with due acknowledgement of collaborative research and discussions. This thesis is a bonafide record of original work done by me and all sources listed within have been detailed in the bibliography.

Pardeep Kumar
(Candidate)

Dated: April 26, 2019

In my capacity as the supervisor of the candidate's project work, I certify that the above statements by the candidate are true to the best of my knowledge.

Dr. Yogesh Singh
(Supervisor)

Acknowledgment

I would like to express my heartfelt gratitude to my supervisor, Dr. Yogesh Singh for his guidance and innovative support. I genuinely appreciate him for giving me an opportunity to work on the exciting problem in the Field of frustrated magnetic system.

I would also like to express my sincere gratitude to my MS committee members, Dr. Sanjeev Kumar and Dr. Goutam Sheet for being in my committee. I would like to acknowledge XRD facility, Clean room facility and SEM facility, Raman spectroscopy facility, AFM facility of IISER Mohali. I am grateful to Vivek Kumar (SEM operator) that he helps in SEM and EDX facility. I appreciate the Financial support provided by DST India and IISER Mohali and for attending the Workshop on Correlated electron system in Julich, Germany. I am grateful to DST India, India for the research fellowship during BS-MS.

I am grateful to all members of Novel Material Lab:- Dr. RK Gopal , Ashiwini, Anzar Ali, Amit, and Shama. I would like to give special thanks to Dr. RK Gopal for guiding me. I am very thankful to Anzar Ali who help in operating the instruments. They help me in during experimental measurement, scientific discussion, operating software.
I would like to thanks to my friends Neetu Lamba, Riyaz ahmad, Avinesh Kumar, S.S Sreenath, Ravi Kumar. for making my years enjoyable at IISER Mohali. From outside the IISER Naveen Yadav, Pankaj Grewal, Shyam Sunder who have always motivated me. My sincere appreciation to my friends, seniors, and all who contributed to the completion of my MS dissertation.

My deepest appreciation to my elder sister Richa Tanwar and my elder brother Sandeep Tanwar for making crazy and joyful moment at home. This MS work would not have been possible without blessing and encouragement of my parents. They have always made sure their children gets the best possible opportunities at every step. I would never be able to return their unconditional love and support. I dedicate my MS thesis to my elder brother Sandeep Tanwar and my parents.

List of Figures

Abstract

This work is divided into two part. In the first part, we have used a liquid exfoliation method to produce quasi two-dimensional (2D) flakes of Kitaev magnets Na_2IrO_3, $(Na_{0.85}Li_{0.15})_2IrO_3$ and $\alpha - RuCl_3$. For this work, existing crystals of Na_2IrO_3 and $(Na_{0.85}Li_{0.15})_2IrO_3$ were used and new crystals of $\alpha-RuCl_3$ were grown. By ultrasonic shaking of these crystals in an LiOH solution in ethanol, we were able to separate them into 2D sheets which are 1-3μm wide and down to 2 nm thick. SEM and AFM characterization, and thickness distribution of these flakes with varying ultrasonic shaking time on these flakes are reported.

In the second part, crystals of $\alpha-$ $RuCl_{3-x}Br_x$ and $\alpha-RuCl_3$ have been synthesized using a self-flux growth method. A thorough chemical and structural characterization of these crystals have been carried out by SEM, EDX and Raman spectroscopy techniques. Magnetization measurements have been performed to probe the magnetic ground state of these crystals. We have observed magnetic transition at T_N= 8 K, 12 K in 4% Br substituted (sheet) and 8% Br substituted (needle) crystals respectively, indicating that the magnetic order of parent α-$RuCl_3$ survives on Br substitution.

Contents

Chapter 1

Introduction

1.1 Kitaev materials

1.1.1 Kitaev model

The Kitaev model is an exactly solvable model for interacting spin S=1/2 on the honeycomb lattice (Figure 1.1). The Kitaev Hamiltonian is written as

$$H = \sum_{<i,j>,\gamma} K_\gamma S_j^\gamma S_k^\gamma$$

where Kiteav exchange K_x, K_y, and K_z are Ising like ferromagnetic coupling between nearest neighbours (NN) [Kitaev 06].

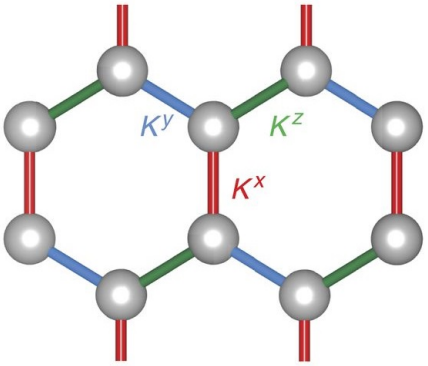

Figure 1.1: Honeycomb lattice showing Kitaev coupling on the three different NN linkage of the lattice (blue, green and red solid line) [Banerjee 17]

1.1.2 Kitaev-Heisenberg (K-H) model

In real materials apart from the anisotropic Kitaev term in the Hamiltonian, there is an isotropic Heisenberg term which was introduced in Kitaev-Heisenberg (KH) model described as:

$$H = -K \sum_{<i,j>,\gamma} S_j^{\gamma} S_k^{\gamma} + J \sum_{<i,j>} S_{\mathbf{J}}.S_{\mathbf{k}}$$

The first-term represents the Kitaev term and the second term represents the isotropic Heisenberg term. K is Ising like ferromagnetic coupling whereas J is the anti-ferromagnetic coupling.
To determine the ground state phase diagram of the KH model, K and J have been parameterized as 2α and (1-α) respectively. The parameterized KH model is [Chaloupka 10]:

$$\mathrm{H}{=}{-}2\alpha{\textstyle\sum_{<i,j>\gamma}} S_j^{\gamma} S_k^{\gamma} + (1-\alpha){\textstyle\sum_{<i,j>}} S_j.S_k.$$

By varying the value of α from 0 to 1 the Hamiltonian changes from pure Heisenberg ($\alpha = 0$) to pure Kitaev $\alpha = 1$. The different ground states obtained as α is varied are shown in (Figure 1.2).

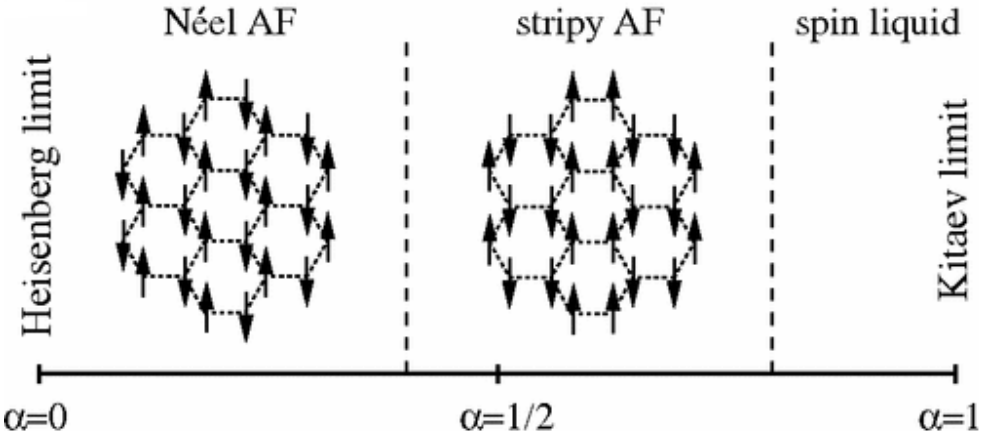

Figure 1.2: Phase diagram of KH model with AF Heisenberg and FM Kitaev [Chaloupka 10].

1.1.3 Kitaev materials

Several 5d and 4d materials have been proposed as candidate Kitaev materials. The most well studies are Na_2IrO_3, α-Li_2IrO_3, and $\alpha{-}RuCl_3$.

1.2 $\alpha-RuCl_3$

Although A_2IrO_3 materials were the first studied Kitaev materials, $\alpha-RuCl_3$ has become important because iridates have a large absorption cross-section for neutron while $\alpha-RuCl_3$ does not, allowing a detailed study of the magnetic excitations.

1.2.1 Crystal structure

$\alpha-RuCl_3$ is built up of honeycomb layers of edge sharing $RuCl_6$ octahedra as stacked along the c-axis to form a 3-D structure. Due to the possibility of different stacking sequence of the honeycomb layers, there exist different crystal structures.
The material crystallizes either in the trigonal space group $P3_112$ or the monoclinic space group C2/m which contain three and one honeycomb layer in each unit cell respectively [Cao 16]. The C2/m structure is shown in figure 1.3. At low temperature (typically 150 K) $\alpha-RuCl_3$ exist in monoclinic crystal structure with a=5.951, b=10.354, c=6.014 (in angstrom), and $\beta = 108.800°$

Figure 1.3: Monoclinic crystal structure (C2/m space group) of $\alpha-RuCl_3$ showing black dashed line as unit cell Ru as red, and Cl as green balls.(a) Represent the layers of $\alpha-RuCl_3$ projected into ab plane and (b) one is the projection in ac plane

1.2.2 Magnetic structure

Previous studies on $\alpha-RuCl_3$ suggested that it has a zigzag magnetic ground state with transition temperature varying between 7 K and 15 K depending upon crystal quality. One can suppress the zigzag magnetic order by applying an in-plane magnetic field. Magnetic ordering disappeared at the field of 8 T and above. The recent study, by neutron diffraction shows that suppression of magnetic ground state leads to a state with a gapped magnetic excitation [Sears 17]. Nature of these gapped excitations close to the critical field of 8T is till a topic of future study [Winter 17].

1.3 Motivation

.

- $\alpha-RuCl_3$, Na_2IrO_3 are magnetically ordered at low temperature and not strictly quantum spin liquids.
  Can we tune these materials towards the Kitaev limit?
- Separating the layers will suppress the inter-layer magnetic exchange and promote possibility of realizing a QSL state.

1.4 Structure of thesis

- Chapter 2: In this chapter, I have described experimental techniques which were used in single crystal synthesis, characterization, and magnetic measurements.
- Chapter 3: Here I have probed magnetization in single crystals of α-$RuCl_{3-x}Br_x$ and $\alpha-RuCl_3$ by SQUID magnetometer.
- Chapter 4 describes the exfoliation of bulk single crystal into quasi 2D flakes of 2-3 μm width and down to 2 nm thick. These flakes are of $\alpha-RuCl_3$, Na_2IrO_3 and $Na_{0.85}L_{0.15})_2IrO_3$ characterized by adopting different characterization techniques, i.e., surface morphology by scanning electron microscope (SEM), chemical composition by energy-dispersive x-rays (EDX), and thickness measurement by atomic force microscopy (AFM), etc. Our attempts to probe magnetization in these flakes by vibrating sample magnetometer (VSM) were unsuccessful.

Chapter 2

Experimental Techniques

In this chapter, we will discuss the experimental techniques which are adopted in crystal growth, characterization, magnetic property measurements, and exfoliation of quasi 2D flakes of single crystals.

2.1 Single crystal synthesis

Single Crystal growth of $\alpha-RuCl_3$ and $\alpha-RuCl_{3-x}Br_X$ was carried out by self-flux method. We have used a box furnace (1500°C) for the single crystal growth process.

Figure 2.1: Box furnace.

2.1.1 Self-flux method

In this method, a solute is mixed with a suitable flux and heated above the melting point of the flux. Solute completely dissolved in flux at this temperature and solution attains super-saturation point. During slow cooling (1-4°C/h) process crystals start to grow. The molten flux is removed by centrifugation . In flux growth, if one of its constituent element act as flux then it called self-flux growth method.

2.1.2 Single crystal synthesis of $\alpha-\mathbf{RuCl_3}$ and $\alpha-\mathbf{RuCl_{3-x}Br_x}$

For crystal growth of $\alpha-\mathrm{RuCl_3}$ and $\alpha-\mathrm{RuCl_{3-x}Br_x}$, we have taken a finite amount of anhydrous $\mathrm{RuCl_3}$, and $RuBr_3$ + $RuCl_3$ powder (99:99 % Alfa Aesar) respectively and vacuum dried in a quartz ampoule at least for 5 hours. Vacuum driying is a crucial step because anhydrous $\mathrm{RuCl_3}$ powder absorbed water from the environment during putting off from the glove box to placing in the quartz ampoule. Then we sealed the quartz ampoule under vacuum.

We put ampoule in box furnace and heated it upto 1050°C in 6 hours and stayed here for 20 hours after which it was cooled to 600°C at a rate of 2°C per hour and quenched with cold water at this temperature. Extraction of a single crystal is a difficult task from the semi-melted powder bed, as they are randomly stacked and found to grow into each other and are very thin. We have got plate-like and needle-shaped black shiny single crystals as shown in Figure 2.2.

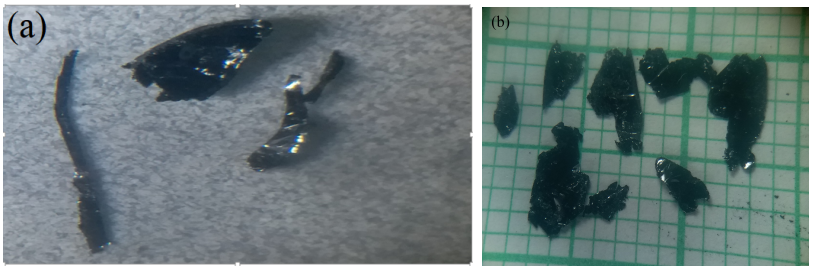

Figure 2.2: (a) $\alpha-\mathrm{RuCl_3}$ (b) $\alpha-\mathrm{RuCl_{3-x}Br_x}$ crystals.

2.2 Chemical Analysis : Energy-dispersive x-ray

Chemical composition of the grown single crystals has been done using energy dispersive x-ray spectroscopy (EDS) on a JEOL scanning electron microscope (SEM). One can determine the chemical composition by characteristic x-ray of its constituent element'smbecause every element has a unique characteristic x-ray energy spectrum.

The EDS measurement using the SEM, it is a two-step process. In the first step, an electron is bombarded with high energy on the target sample which excits the electrons

of the target sample to there higher energy shells. In the second step, the excited electron giving x-rays of the energy difference between the transition shells. A photo-detector detects these x-rays. The composition of the material can be quantified very precisely.

2.3 Raman spectroscopy

Raman spectroscopy uses an inelastic scattering in which light interacts with matter and acts as a probing tool. In this, monochromatic laser light with finite frequency excites molecules and transforms them into oscillating dipoles. Such oscillating dipoles emit light of different frequencies than the incident light. Lower energy photon emitted gives Stoke lines and higher energy photon emitted gives anti-Stokes lines. Each peak in Raman spectra corresponds to a specific molecular bond vibration called Raman phonon mode [Ram].

2.4 Magnetic measurement: Vibrating sample magnetometer (VSM)

VSM is a versatile technique to probe magnetic properties with magnetization changes of less than or equal to 10^{-6} emu. In VSM the sample is made to move up and down with the help of linear motor. When there is a change in flux during the moving process this change is detected by the pickup coil shown in figure 2.3 [Mehlawat 18]. Pickup coil has a special design so that it can cancel out its own flux and detect the change in magnetic flux due to sample only. This change in flux induces a time-dependent voltage in pickup coil. Induce voltage is amplified by an amplifier and converted into the magnetic moment of the sample by below equations:

$$V_{coil} = (\frac{\partial \Phi}{\partial z})(\frac{\partial z}{\partial t})$$

where Φ is flux enclosed in coil, z is vertical position of a sample while taking reference from pickup coil, t is time.
Voltage generated in pickup coil for sinusoidally oscillating sample is:

$$V_{coil} = 2\pi f C m A \sin(2\phi f t)$$

where C, m, A, and F are coupling constant, magnetic moment (DC) of the sample, amplitude of oscillation, and frequency of oscillation respectively [VSM 08].

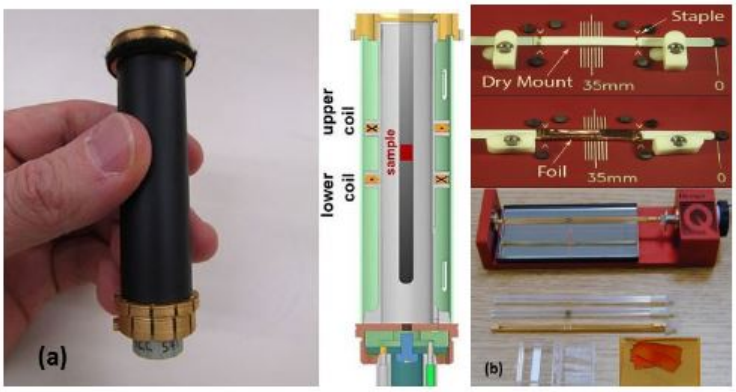

Figure 2.3: (a) VSM pickup coil and its schematic representation (b) sample mounting plateform [Mehlawat 18].

2.5 Exfoliation: Liquid exfoliation technique

We have exfoliated bulk single crystals by liquid exfoliation technique. In this technique, a small amount of single crystals (typically 15-20 mg) are placed in a suitable solvent in the presence of an intercalating agent. Intercalating agent accommodated between the layers of a layered crystal. By ultrasonically shaking layers are expected to separate. Longtime settlement of layers leads to monolayer or few monolayer's nanosheets on top of solvent. The sheets can be extracted by the drop-casting the solvent onto an inert substrate like Si.

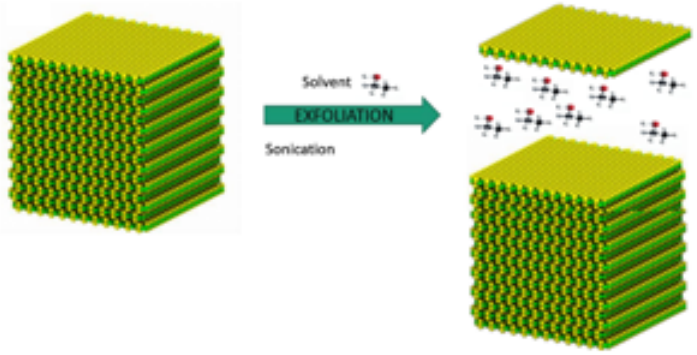

Figure 2.4: Liquid exfoliation technique

2.6 Atomic force microscope (AFM)

Atomic Force Microscopy (AFM) is a versatile technique for measuring the thickness of mesoscale and nanoscale sample. AFM is capable of sensing the force of atomic order. The cantilever in AFM climbs with a tip as shown in Figure 2.5. This tip senses the atomic level interaction force.

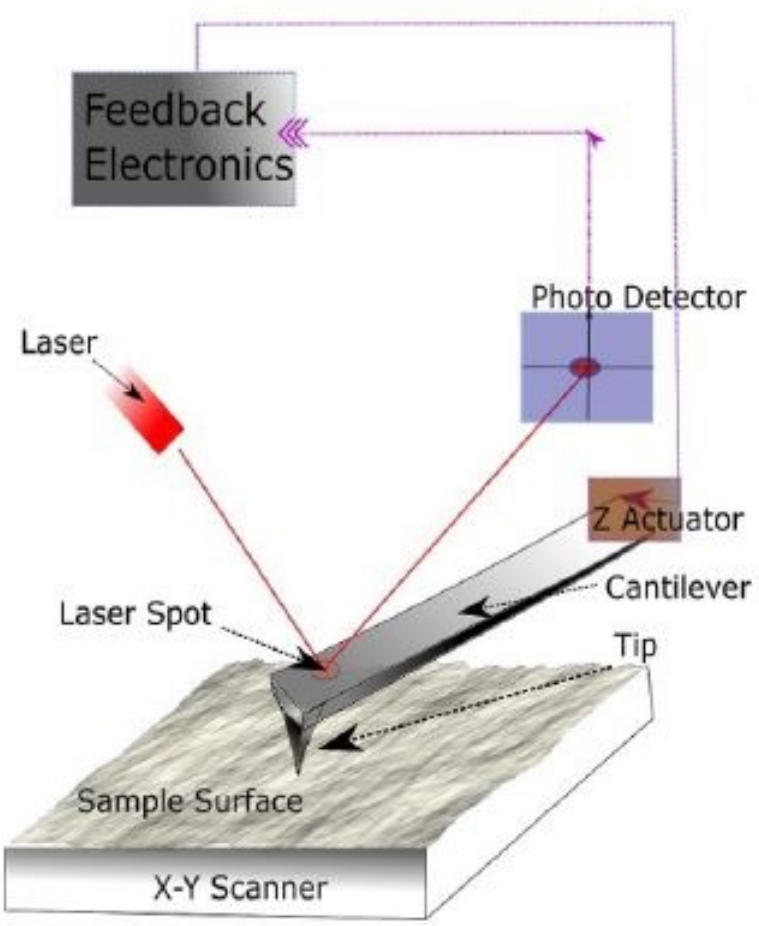

Figure 2.5: Schematic of an AFM [L.Yadav 18].

The interaction force which is induced from inter-atomic forces or any electromagnetic forces causes a deflection in laser light which is falling on it during the work process. This change in deflection is detected by photo-detector which has four quadrants (Figure 2.6) that generate voltage upon falling of light intensity. Initially, the laser spot is centered at origin all quadrant. Deflection in cantilever changes the position of the centered laser spot, and the voltage difference is calculated from the generated voltage in the upper-lower quadrant, or left-right quadrant gives vertical and lateral deflection respectively.

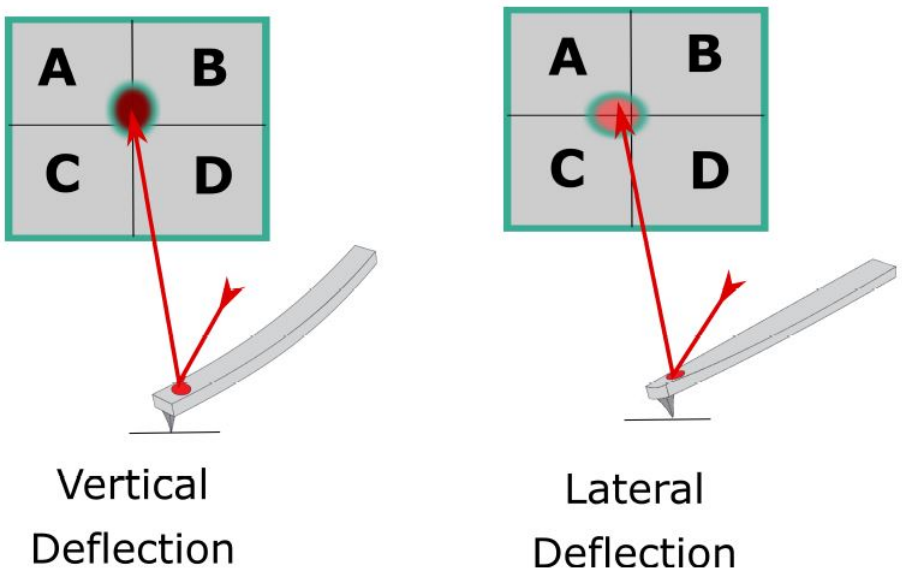

Figure 2.6: Vertical and Lateral deflection detection by generated voltage [L.Yadav 18].

In non-contact mode, cantilever oscillates at resonates frequency and amplitude of oscillation kept constant during the scanning of a sample surface. This mode is based on the feedback mechanism and effective change in resonating frequency act as a feedback parameter. Constant amplitude is maintained by feedback parameter which leads to variation in the vertical position of the tip. The control signal regulates the tip position and provides information on thickness as shown in Figure 2.7.

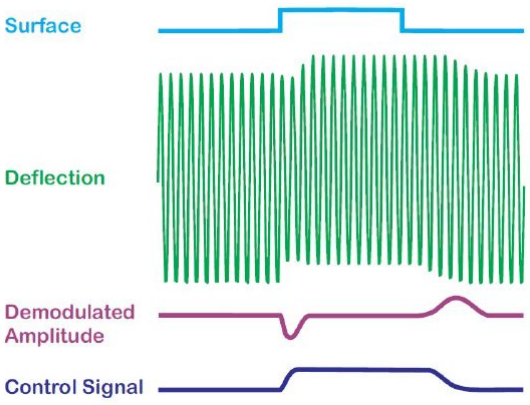

Figure 2.7: Signal detection in non-contact or AC mode [L.Yadav 18].

Chapter 3

Crystal Growth and Magnetic property measurements: $\alpha-\mathbf{RuCl_3}$ and $\alpha-\mathbf{RuCl_{3-x}Br_x}$

3.0.1 Crystal growth

We have grown $\alpha-\mathrm{RuCl_3}$ by a self-flux growth method which is briefly described in section 2.1.2. We have taken 0.5g amount of anhydrous α-RuCl_3 and placed it in a quartz tube with one end moulded in v-shaped . The v-shaped end of the quartz tube provides a contact or starting point for nucleation of the single crystals in the crystal growth process. There is a possibility of absorbing water from the environment while placing the sample in the quartz tube. To remove this possibility, we have thoroughly dried the tube in vacuum at 250°C for 4-5 hours, which is above the vaporization temperature of water. This is a crucial step in the crystal growth process. If the sample is not properly dried in the vacuum thoroughly then at the high temperature of 1075°C vapor of water exert a high pressure at the walls of quartz tube which is out of the capacity of tube. An explosion of the tube might occur which may damage the furnace.

A similar process is used to grow the crystals of α-$\mathrm{RuCl_{3-x}Br_x}$. For growing crystal, we took 0.1g of anhydrous $\mathrm{RuBr_3}$ and 0.9g of anhydrous $\mathrm{RuCl_3}$ powder in the quartz tube and vacuum dry the tube thoroughly. After following the self-flux method, we get needle-shaped and plate-like crystals of α-$\mathrm{RuCl_{3-x}Br_x}$ which contained approximately 7-8% and 2-4% of Br concentration respectively. Temperature profile which was followed in crystal growth shown in Figure 3.1.

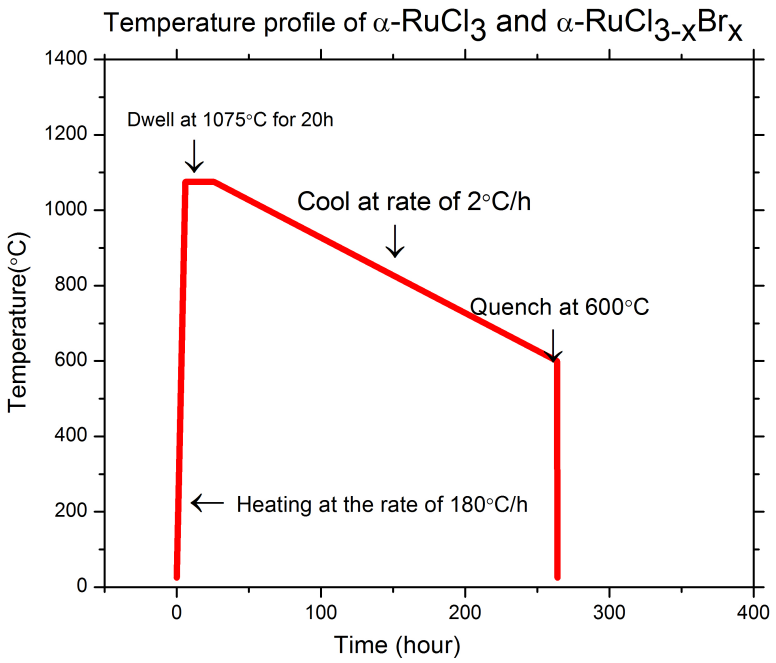

Figure 3.1: Temperature profile.

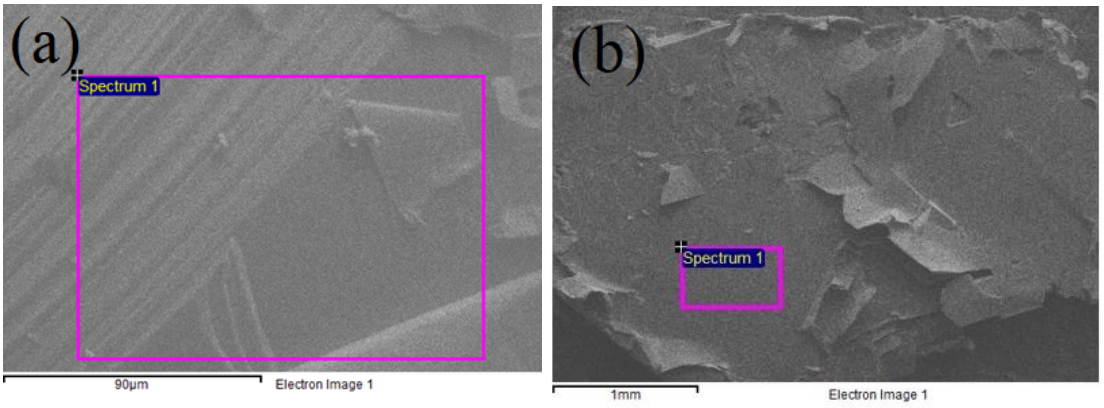

Figure 3.2: SEM image of (a) $\alpha-RuCl_3$ (b) α-$RuCl_{3-x}Br_x$ crystals.

3.0.2 Characterization: EDX

Chemical composition analysis was performed by the energy dispersive X-ray technique (EDX) in SEM (JEOL Ltd). We have got the exact chemical composition that we are expecting (Figure 3.2(a)). The EDX spectrum data of both crystals show the presence of the expected elements (Figure 3.3(b) and 3.4(b)). We have calculated the value of x in

different crystals of α-$RuCl_{3-x}Br_x$ from chemical composition provided by EDX. Value of x varying from 0.085 to 0.36 (Figure 3.4(a), 3.4 and 3.6).

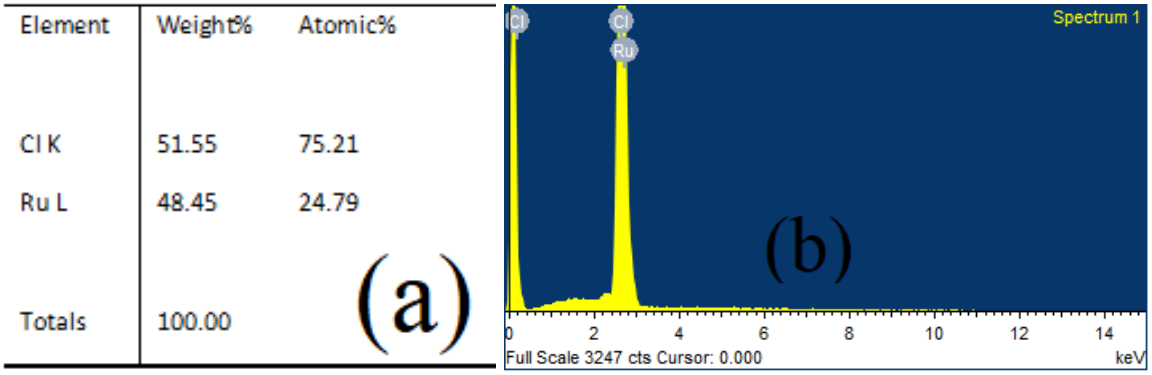

Figure 3.3: (a) Chemical composition with $x = 0$ (b) EDX spectra of $\alpha-RuCl_3$.

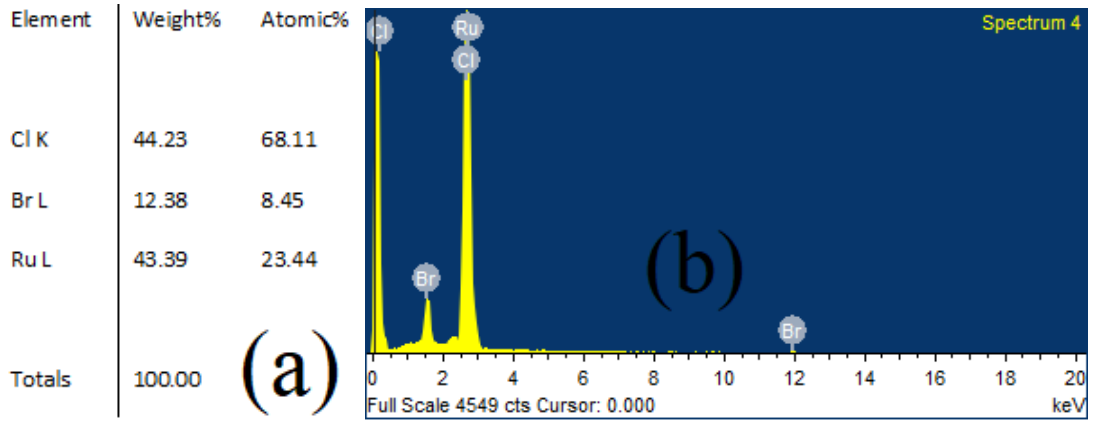

Figure 3.4: (a) Chemical composition with $x = 0.36$ (b) EDX spectra of α-$RuCl_{3-x}Br_x$.

Element	Weight%	Atomic%
Cl K	50.87	74.38
Br L	3.12	2.02
Ru L	46.01	23.60
Totals	100.00	

(a)

Element	Weight%	Atomic%
Cl K	50.42	73.75
Br L	5.96	3.87
Ru L	43.62	22.38
Totals	100.00	

(b)

Element	Weight%	Atomic%
Cl K	47.97	71.75
Br L	6.86	4.55
Ru L	45.17	23.70
Totals	100.00	

(c)

Figure 3.5: Chemical composition with (a) $x = 0.085$ (b) $x = 0.17$ and (c) $x = 0.191$ in α-$RuCl_{3-x}Br_x$.

Element	Weight%	Atomic%
Cl K	48.44	72.04
Br L	7.66	5.05
Ru L	43.90	22.91
Totals	100.00	

(a)

Element	Weight%	Atomic%
Cl K	45.17	69.25
Br L	8.86	6.03
Ru L	45.96	24.72
Totals	100.00	

(b)

Element	Weight%	Atomic%
Cl K	45.24	69.16
Br L	10.36	7.03
Ru L	44.40	23.81
Totals	100.00	

(c)

Figure 3.6: Chemical composition with (a) $x = 0.220$ (b) $x = 0.245$ (c) $x = 0.297$ in α-$RuCl_{3-x}Br_x$.

3.0.3 Magnetic susceptibility measurement on a α-$RuCl_3$ single crystal

Magnetization measurements on these crystals were carried out in a SQUID magnetometer at a field of 1 T. We have plotted the molar magnetic susceptibility in the temperature range (2K to 300 K) using OriginPro 8.5 software (Figure 3.6). From the data on the inset it is clear that our crystals shows two transition at 7 K and 14 K. This suggests the presence of significant amount of stacking fault in crystals [Sears 17].

The $1/\chi_m$(T) data between T = 100K to 300 K were fitted by the Curie-Weiss expression $1/\chi_m(\mathrm{T}) = 1/\ (\chi_0 + C/\mathrm{T}\text{-}\theta_{cw})$, where χ_0 , C, and θ_{cw} are fitting parameters. These parameters values were found to be χ_0= -1× 10^{-4}, $C = 0.3578\ cm^{-3}mol^{-1}K$ and $\theta_{cw} = 78$ K.

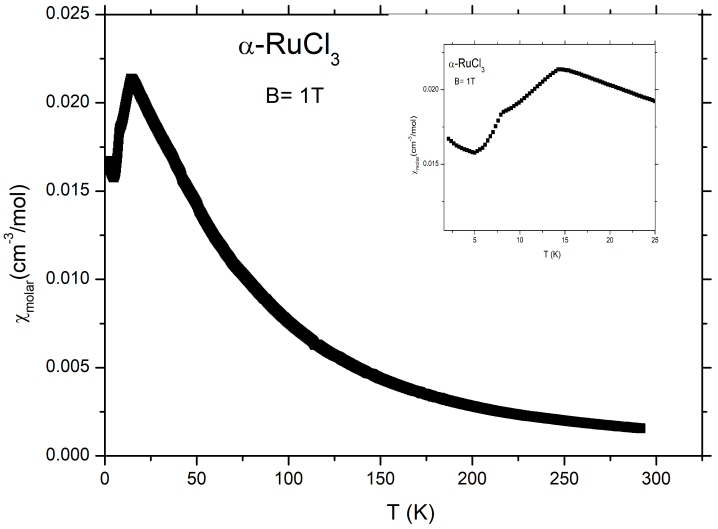

Figure 3.7: Molar magnetic susceptibility(χ_m) vs. temperature (T) at a magnetic field of 1 T. Inset shows χ_m in temperature range of 2 K to 25 K.

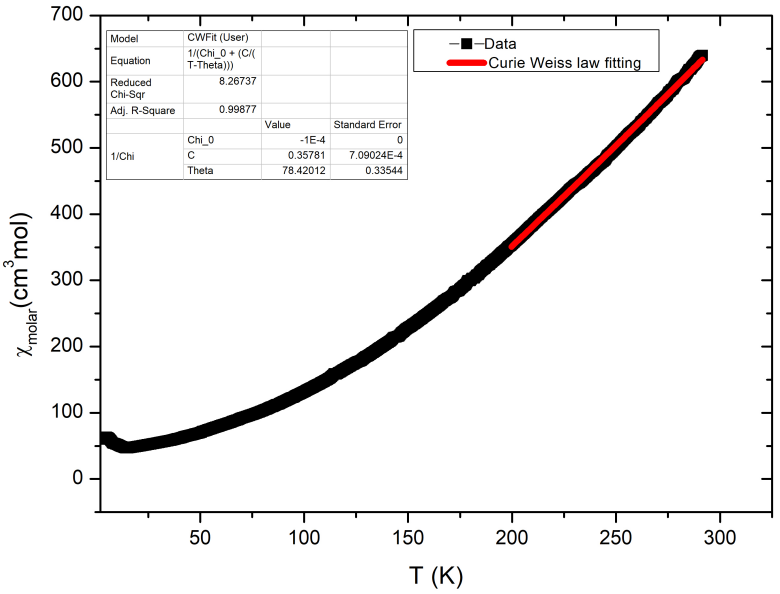

Figure 3.8: The plot of $1/\chi_m$ vs. T(K) at a field of 1 T where a solid red line represents fitting Curie-Weiss behavior in the paramagnetic region. Inset shows the fitting parameters.

3.0.4 Magnetic susceptibility measurement on a single crystal of α-$RuCl_{3-x}Br_x$

Magnetic susceptibility of α-$RuCl_{3-x}Br_x$, shows a possible magnetic transitions at $T \simeq 8$K and $T \sim 12$K for plate-like crystals with $x \sim 4\%$ and needle-shaped crystals with 8% Br (Figure 3.9 and 3.11).

The value of fitting parameters was calculated by plotting $1/\chi_m$ vs. T in a temperature range of 100 K to 300 K, which is shown in Figure 3.10 and fitting with Curie-Weiss law expression. The values of these parameters were found to be χ_0= -1× 10^{-4}, $C = 0.65789$ $cm^{-3}mol^{-1}K$ and $\theta_{cw} = 30$ K.

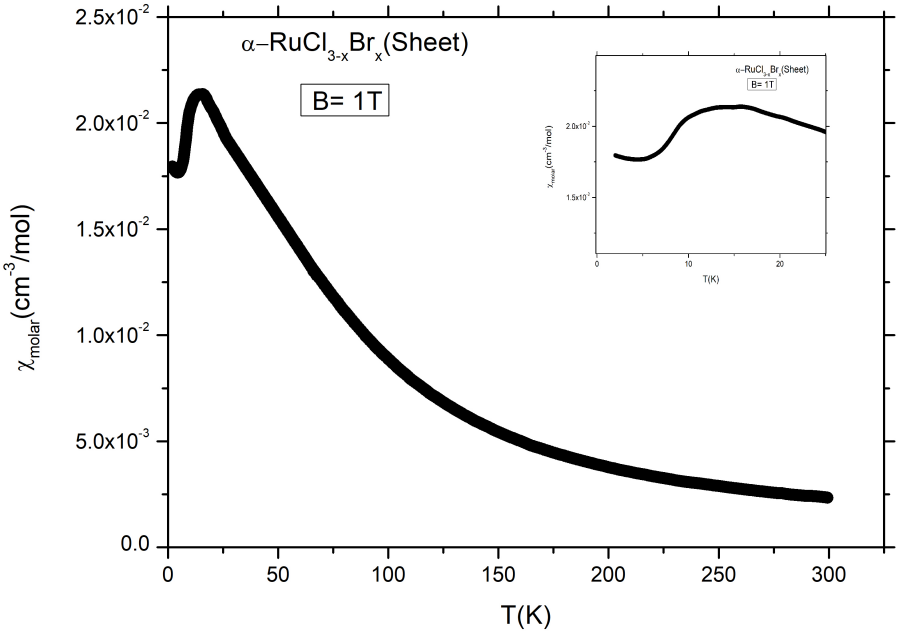

Figure 3.9: Plot of molar magnetic susceptibility(χ_m) vs. temperature at a magnetic field of 1 T of α-$RuCl_{3-x}Br_x$ with $x = 5.78$. Inset shows χ_m in temperature range of 2 K to 25 K.

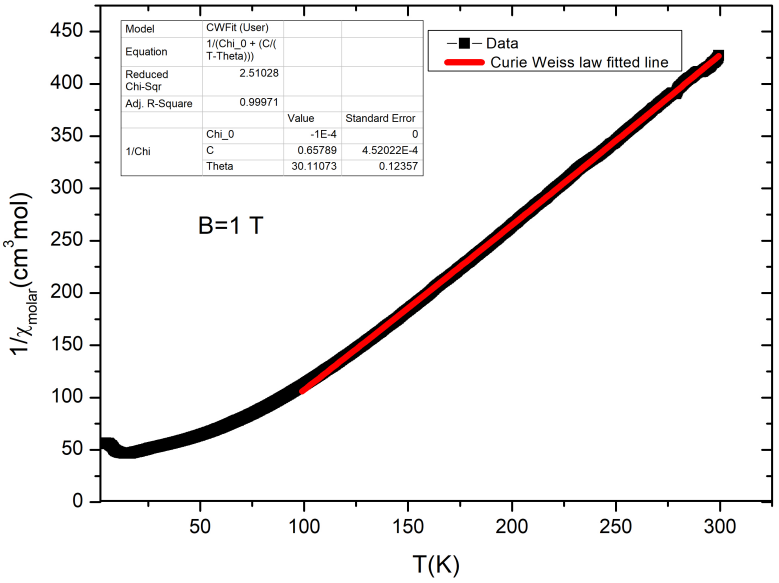

Figure 3.10: The plot of $1/\chi_m$ vs. T(K) at a field of 1 T and the solid red line represents fitting Curie-Weiss behavior in the paramagnetic region. Inset shows the fitting parameter.

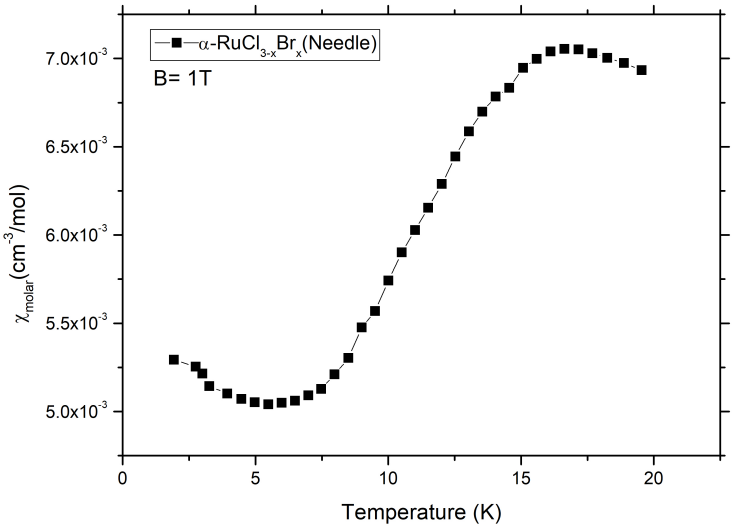

Figure 3.11: Plot of molar magnetic susceptibility(χ_m) vs. temperature at a magnetic field of 1 T in temperature range of 2 K to 20 K for needle-shaped α-$RuCl_{3-x}Br_x$.

3.1 Structural information from Raman spectroscopy

3.1.1 $\alpha-RuCl_3$ and α-$RuCl_{3-x}Br_x$ crystals

We have taken the Raman spectra with the 514 nm laser at a magnification of 100x and 10 sec accumulation time. Raman spectra of $\alpha-RuCl_3$ shows 7 phonon-modes. This is consistent with previously reported data [Zhou 18]. The α-$RuCl_{3-x}Br_x$ crystals also show a similar Raman spectra, suggesting that the $\alpha-RuCl_3$ structure is also adopted by the Br substituted crystals.

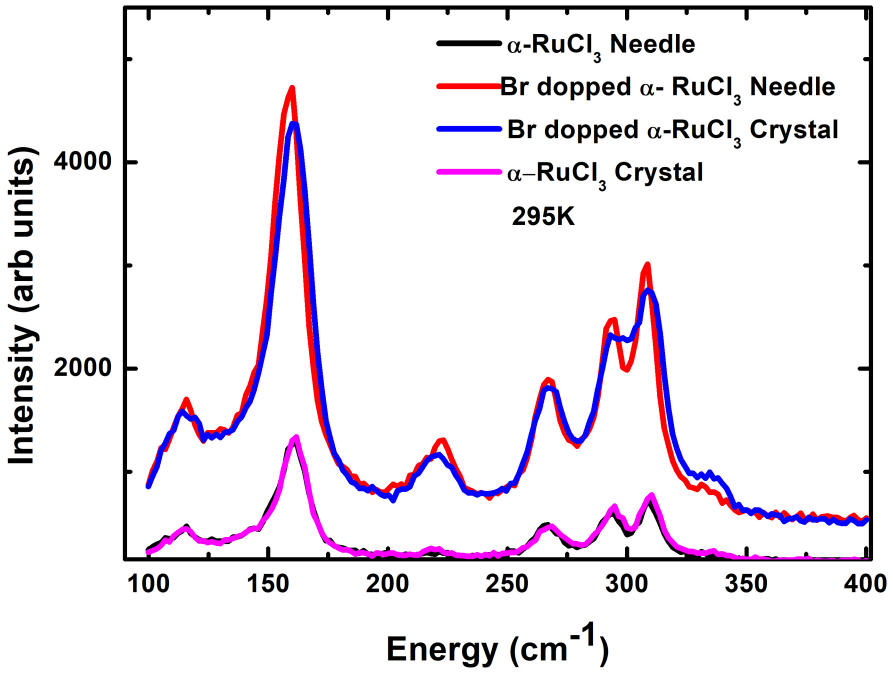

Figure 3.12: Pink, black, blue and red spectrums show Raman spectra of plate-like α-$RuCl_3$, needle-shaped α-$RuCl_3$, plate-like α-$RuCl_{3-x}Br_x$ and needle-shaped α-$RuCl_{3-x}Br_x$ single crystal respectively.

3.2 Discussion

Detailed structural investigation of α-$RuCl_{3-x}Br_x$ need more sensitive techniques like single XRD (x-ray diffraction) to determine stacking disorder and crystalline phase purity and thermal detailed magnetic studies on Br substituted sample needs to be done in future to track changes in transition temperature.

Chapter 4

Liquid exfoliation of Kitaev Magnets

4.1 Introduction

Previous studies on Kitaev materials suggested that the candidate materials Na_2IrO_3, $(Na_{0.85}L_{0.15})_2IrO_3$, and $\alpha-RuCl_3$ are not in the strictly quantum spin liquid regime because these materials show a magnetic order at low temperatures. K-H model suggests that there is a Heisenberg isotropic magnetic exchange apart from Kitaev magnetic exchange in these materials. These materials form a honeycomb lattice via edge-sharing octahedra and there exits three super-exchange paths. For cancellation of isotropic magnetic exchange interaction exactly, there must be an angle of 90° in the super-exchange path of these materials. If there exists any deviation from 90°, the isotropic magnetic exchange survives which in turn suppresses the possibility of realizing the QSL state [Chaloupka 10].
To suppress inter-plane interaction, we attempted to separate two-dimensional flakes from the as-grown single crystals by liquid exfoliation technique.

Another important reason to study these materials in mono-layer limit or low dimension limit is that these materials have graphene-like mono-layer with SOC and may show graphene-like properties.

4.2 Exfoliation of single crystal: Na_2IrO_3, $(Na_{0.85}L_{0.15})_2IrO_3$, and $\alpha-RuCl_3$

We have exfoliated the single crystals of these materials into Quasi 2D flakes of width 1-3μm and the thickness down to 2 nm, which contains approximately three units cells. For exfoliation, we have taken 15 mg amount of target material's single crystals and kept them

in ethanol solvent in the presence of 2mg of intercalating agent LiOH. This solution is kept undisturbed for 4-5 hours. During this period, intercalating agent intercalates between the layers of target crystals and weakens the inter-layer van der Waal forces. After this, we place the crystal containing solution in the ultra-sonication bath and sonicate this for 3-4 hours in distilled ice water. This is done to avoid heating of solution containing the layers of crystals. Now, we keep this solution for over-night for settling the dense layers. On next day, we carefully poured the supernatant in centrifugable plastic tube and centrifuged it for a finite time (typically half an hour). By this centrifuging process, we hasten the settle down the process. After this, we again keep the as prepared solution over-night undisturbed. This solution contains monolayers and few layer shetts at the top of the surface of the solution. We carefully extract these layers with the help of a micropipette by drop-casting the solution on a suitable substrate. To avoid oxidation of these separated layers, the drop-casting process was performed in the presence of Ar gas.

4.3 Characterization of flakes: SEM

We have characterized the surface morphology of extracted flakes on Si substrate by SEM (JEOL Ltd). Bulk single crystals are Mott-insulators, and due to the insulating nature, characterization of flakes is quite tricky. Flakes are only visible at low voltage. Here the voltage is an essential parameter in the characterization of such insulating flakes. We have set the voltage in the range of 2-5 kV and working distance in the range of 6-12 mm.

4.3.1 $\alpha-\mathbf{RuCl_3}$

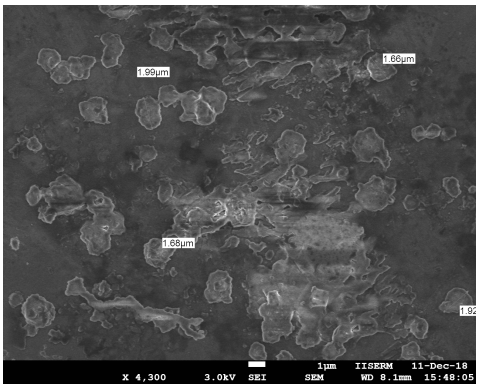

Figure 4.1: Bright spots are quasi 2D flakes on grey black background of Si substrate after drop-casting 5 times

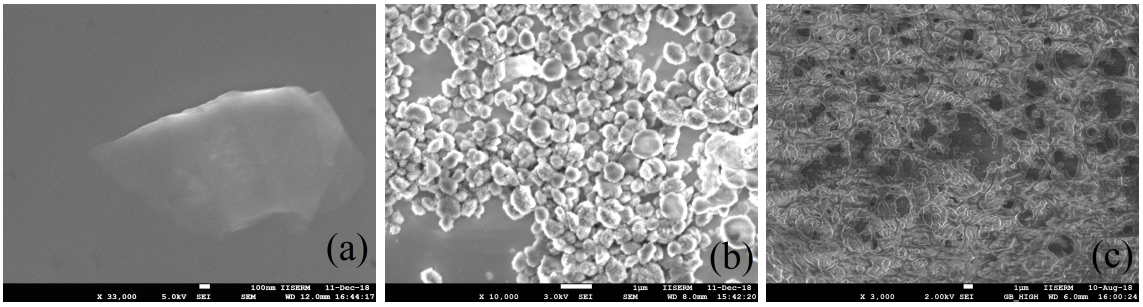

Figure 4.2: (a) Nano-sheet (b) and (c) Quasi 2D flakes on grey black background of Si substrate with 2, 10 and 500 times drop-casting respectively.

4.3.2 Na_2IrO_3

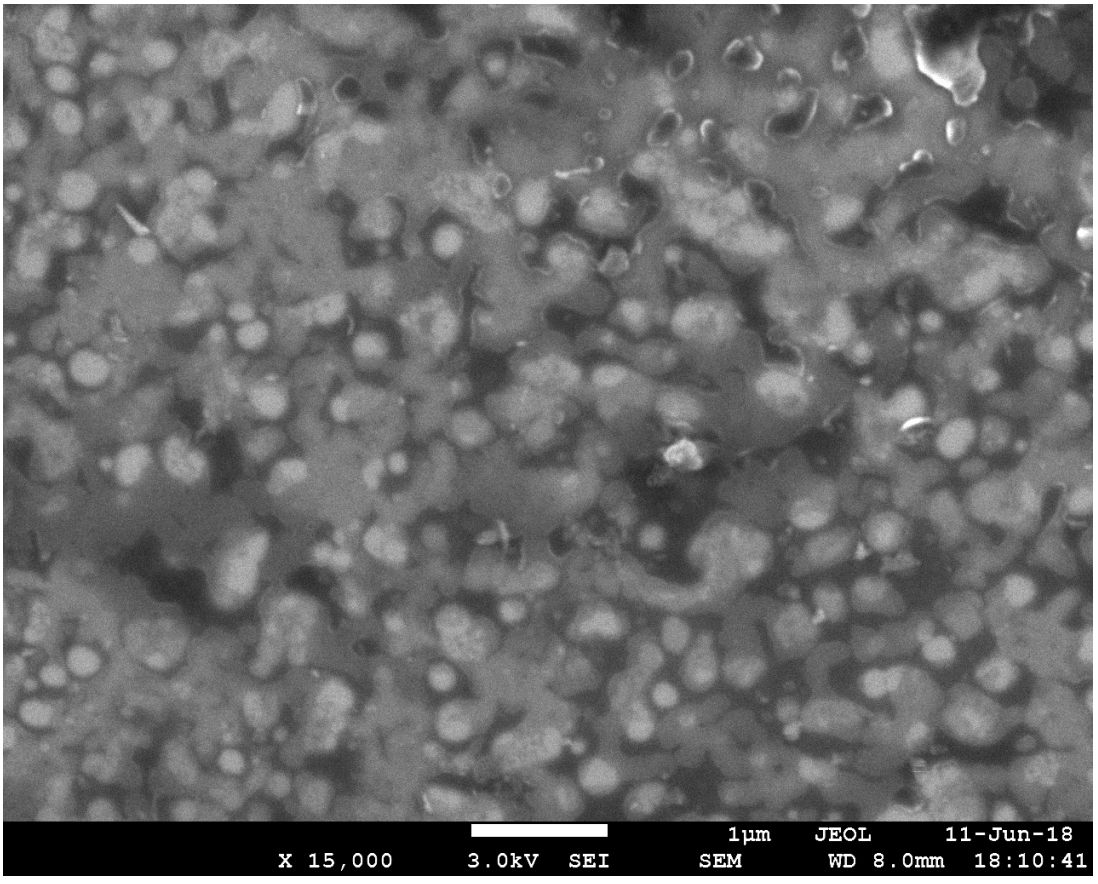

Figure 4.3: Bright spots are quasi 2D flakes on grey black background of Si substrate with 100 times drop-casting.

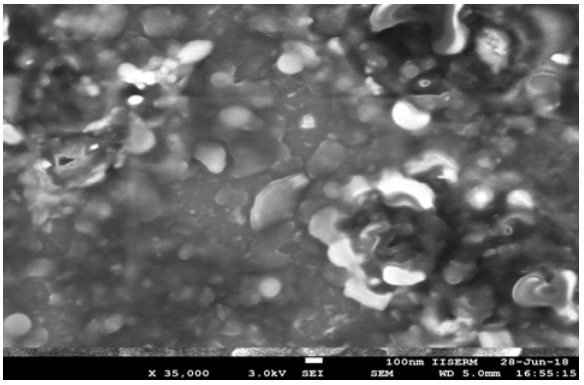

Figure 4.4: Bright spots are quasi 2D flakes on grey black background of Si substrate with 10 times drop-casting.

4.3.3 $(Na_{0.85}L_{0.15})_2IrO_3$

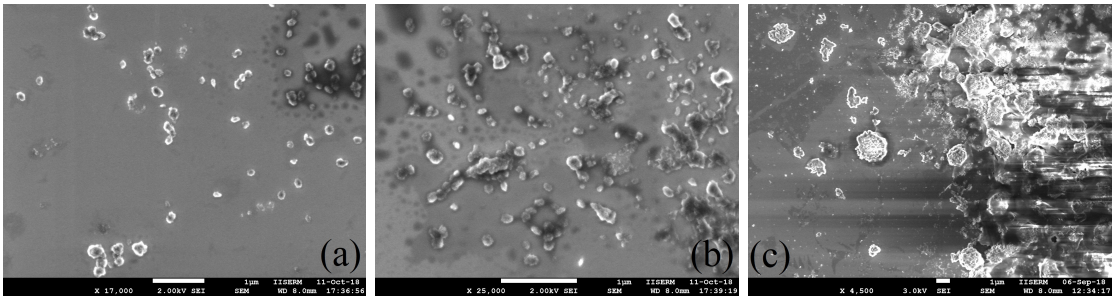

Figure 4.5: (a)-(c) Quasi 2D flakes on grey black background with 5 times drop-casting on three different Si substrates.

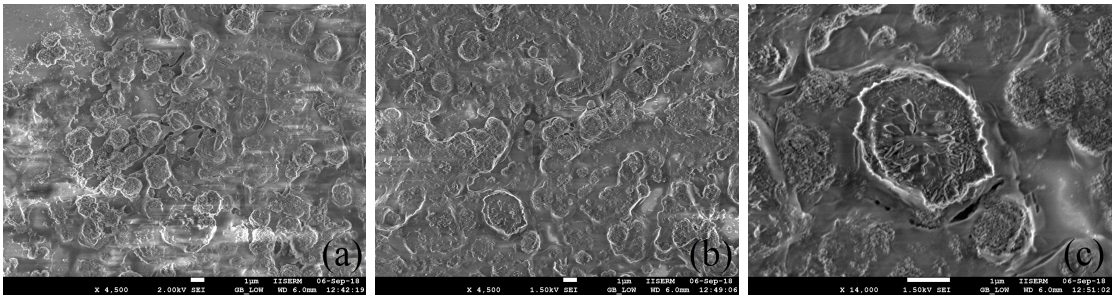

Figure 4.6: (a)-(c) Thick quasi 2D flakes on grey black background with 5 times drop-casting on three different Si substrates.

4.3.4 Chemical composition: EDX

Chemical analysis of these flakes was carried out by EDX in SEM (JEOL Ltd). EDX was performed at 20 kV voltage. We have faced a problem in this process because these flakes are not clearly visible at this high voltage. We have clearly observed all expected element in EDX spectra, which is shown in the (Figure 4.7). However a quantification of the relative atomic fraction was not possible.

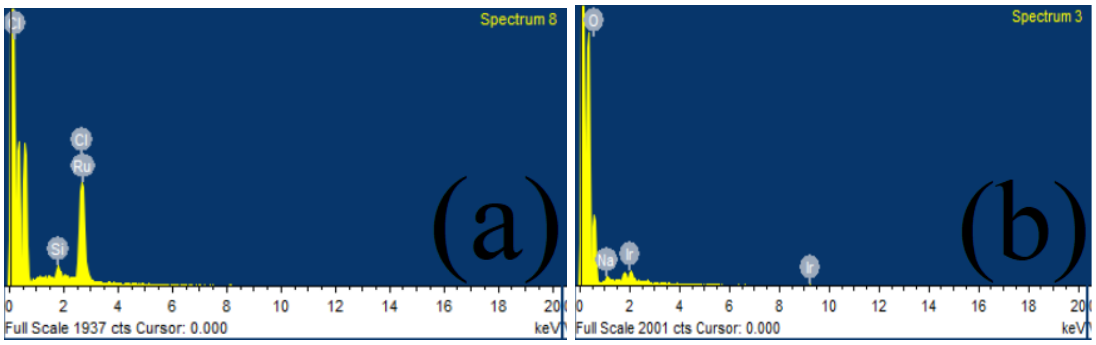

Figure 4.7: EDX spectrum of quasi flake (a) $\alpha-RuCl_3$ (b) Na_2IrO_3 on Si substrate.

4.3.5 Thickness measurement of the flakes: AFM

We have measured the thickness of the flakes by AFM technique in non-contact or AC mode, which is briefly described in section 2.7. After measuring the thickness of 100 flakes, we have plotted a thickness distribution histogram which shows that flakes have a thickness in the range of 2nm to 60nm (Figure 4.8 and 4.9). Negative height because we set h=0 at the top of a flake. When the tip steps down from the flakes it measures h= -ve.

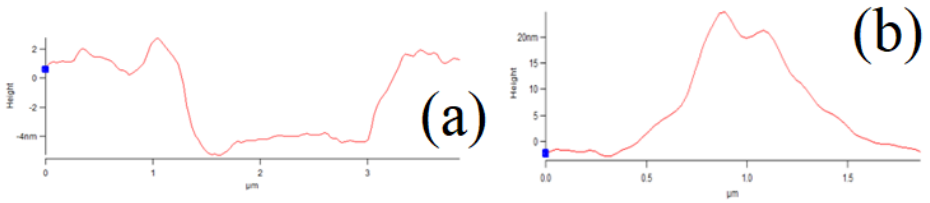

Figure 4.8: 2D layer of Na_2IrO_3 of approximate thickness (a) 2 nm (b) 20 nm.

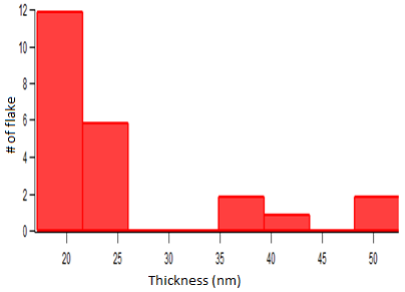

Figure 4.9: Thickness distribution of approximately 100 flakes at 3 hours sonication time.

4.4 Thickness measurement with varying sonication time

We have measured the thickness distribution of these flakes with varying the sonication time. We have exfoliated these flakes on Si substrate by drop-casting the solution five times, keeping the time interval of successive drop-casting at least 2 minutes. The thickness of these flakes is again measured by the AFM technique and the distribution of the thickness has been shown in the (Figure 4.10). A large number of flakes are confined in a short range of thickness with increasing the sonication time.

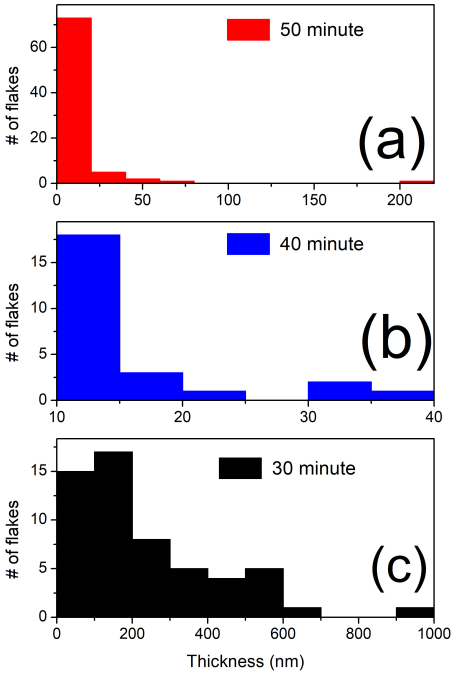

Figure 4.10: Thickness distribution of flakes with varying sonication time (a) 50 minute (b) 40 minute (c) 30 minute.

4.5 Magnetic measurement

We have tried to measure the magnetic susceptibility of quasi 2D flakes of $\alpha-RuCl_3$ and Na_2IrO_3 by vibrating-sample magnetometer (VSM) setup in PPMS-Quantum design. But we have been not able to measure the magnetic susceptibility of these nano-flakes because the value of the magnetic moment is too low (lower than VSM-PPMS resolution range). The measured susceptibility was dominated by the diamagnetism of the substrate .

4.6 Discussion and result

We have tuned the thickness of exfoliated flakes by varying the sonication time (shown in Figure 4.10). We can tune the lateral length of flakes by increasing the amount of intercalating.

Magnetization measurements could not resolve the susceptibility of these flakes and require more sensitive measurements.

Bibliography

[Banerjee 17] Arnab Banerjee, Jiaqiang Yan, Johannes Knolle, Craig A Bridges, Matthew B Stone, Mark D Lumsden, David G Mandrus, David A Tennant, Roderich Moessner & Stephen E Nagler. *Neutron scattering in the proximate quantum spin liquid α-RuCl3.* Science, vol. 356, no. 6342, pages 1055–1059, 2017.

[Cao 16] H. B. Cao, A. Banerjee, J.-Q. Yan, C. A. Bridges, M. D. Lumsden, D. G. Mandrus, D. A. Tennant, B. C. Chakoumakos & S. E. Nagler. *Low-temperature crystal and magnetic structure of* $\alpha - \mathrm{RuCl_3}$. Phys. Rev. B, vol. 93, page 134423, Apr 2016.

[Chaloupka 10] Jiří Chaloupka, George Jackeli & Giniyat Khaliullin. *Kitaev-Heisenberg model on a honeycomb lattice: possible exotic phases in iridium oxides A 2 IrO 3.* Physical review letters, vol. 105, no. 2, page 027204, 2010.

[Kitaev 06] Alexei Kitaev. *Anyons in an exactly solved model and beyond.* Annals of Physics, vol. 321, no. 1, pages 2–111, 2006.

[L.Yadav 18] L.Yadav. Imaging, spectroscopy and device fabrication using scanning probes. IISER Mohali, 2018.

[Mehlawat 18] Kavita Mehlawat. Crystal growth and magnetic property study of layered honeycomb materials with kitaev-like interactions. IISER Mohali, 2018.

[Ram] https://oceanoptics.com/measurementtechnique/raman-spectro.

[Sears 17] J. A. Sears, Y. Zhao, Z. Xu, J. W. Lynn & Young-June Kim. *Phase diagram of* $\alpha-\mathrm{RuCl_3}$ *in an in-plane magnetic field.* Phys. Rev. B, vol. 95, page 180411, May 2017.

[VSM 08] Vibrating sample magnetometer (vsm) option users manual. 2008.

[Winter 17] Stephen M Winter, Alexander A Tsirlin, Maria Daghofer, Jeroen van den Brink, Yogesh Singh, Philipp Gegenwart & Roser Valenti. *Models and materials for generalized Kitaev magnetism*. Journal of Physics: Condensed Matter, vol. 29, no. 49, page 493002, 2017.

[Zhou 18] Boyi Zhou, Yiping Wang, Gavin B Osterhoudt, Paula Lampen-Kelley, David Mandrus, Rui He, Kenneth S Burch & Erik A Henriksen. *Possible structural transformation and enhanced magnetic fluctuations in exfoliated α-RuCl3*. Journal of Physics and Chemistry of Solids, 2018.